DIGITAL INSPECTION OF FIXED CURVIC COUPLING CONTACT PATTERN

A Thesis

presented to

the Faculty of California Polytechnic State University,

San Luis Obispo

In Partial Fulfillment

of the Requirements for the Degree

Master of Science in Industrial Engineering

by

Bradley James Nielson

March 2012

COMMITTEE MEMBERSHIP

TITLE:	DIGITAL INSPECTION OF FIXED CURVIC COUPLING CONTACT PATTERN
AUTHOR:	Bradley James Nielson
DATE SUBMITTED:	March 2012
COMMITTEE CHAIR:	Dr. Daniel J. Waldorf, Professor, Industrial and Manufacturing Engineering
COMMITTEE MEMBER:	Dr. Jose Macedo, Professor, Industrial and Manufacturing Engineering, Department Chair
COMMITTEE MEMBER:	Dr. Sema E. Alptekin, Professor, Industrial and Manufacturing Engineering, Director, Honors Program

ABSTRACT

DIGITAL INSPECTION OF FIXED CURVIC COUPLING CONTACT PATTERN

Bradley James Nielson

This report focuses on providing a foundation for further investigation into the inspection of fixed CURVIC coupling contact pattern by way of modern metrology techniques. Previous bodies of research have utilized coordinate measuring machines (CMMs) to analyze specific features of these couplings, but not the interaction between mating couplings at the areas of contact. It is hoped that this report will provide a basis for further research to improve the efficiency and reduce the ambiguity inherent in the current contact pattern inspection technique. This report contains a comparison between the results of traditional contact pattern inspection and those obtained by CMM. Test couplings were designed, manufactured, and inspected at California Polytechnic State University, San Luis Obispo (Cal Poly). Methods used show a correspondence between the calculated distance between regressed surfaces and the amount of transfer seen from tooth to tooth, but are unable to provide the resolution necessary to make any determinations of what that contact may look like across one tooth surface.

TABLE OF CONTENTS

LIST OF TABLES

LIST OF FIGURES

Chapter 1: Introduction

1.1 Problem Statement

The Fixed CURVIC Coupling, developed by The Gleason Works, is a precision face spline that provides accurate alignment, precision centering, and positive drive between multiple mating components. This coupling is used in gas turbine engines and machine tools which require modular design for assembly and replacement of components, while maintaining the assembly's ability to perform as if manufactured from one piece.

Currently, inspection of production couplings is done by physically seating a production master coupling of the appropriate complementary geometry, coated in a thin film of engineering blue, to the newly produced coupling and observing the transfer pattern of the film to determine if satisfactory contact is made between the two pieces. Each production master is periodically checked by this method to a grand master, which in turn is periodically checked against a gold master to reduce errors associated with wear caused by contact.

This method of inspection fails to directly compare the produced coupling to the intended design. In organizations where multiple masters are needed to support manufacturing, slight variations in shape will produce a different contact pattern depending on which master is used. This method of using masters to inspect manufactured gears also fails to address the fact that it is the interaction between two manufactured gears, not the interaction with a master that will see service [16]. In order to reduce errors and variation it is necessary to compare directly to the intended design and provide the ability to analyze the behavior of two manufactured couplings.

Utilizing a digitally recreated model of the coupling for comparison against a digitally stored engineering model will provide consistency in production, eliminate the need for physical masters thereby removing the cost associated with production and maintenance of master gage sets, and reduce the burden on operators that currently need to skillfully seat masters for proper transfer of engineering blue.

1.2 Purpose and Scope

The purpose and scope of this report is to investigate the feasibility of adapting modern metrology techniques to the inspection of Fixed CURVIC Couplings, with a primary focus on determining contact pattern between mating features. This will include:

- Examination of CURVIC coupling geometry.
- An investigation into using Coordinate Measuring Machines (CMMs) to measure gear geometry.
- Adaptation of these methods for use in estimating contact pattern between CURVIC couplings.
- Design and production of a CURVIC coupling for testing purposes.
- Contact pattern measurement using current method of ink transfer.
- Experimental use of CMM for generating measurement data to be used for estimating contact pattern.
- Comparison of the results from both methods and suggestions for further research.

1.3 Outline of Investigation

The following chapter consists of an investigative look at the current method of CURVIC coupling inspection, as well as how advanced metrological concepts are being applied to gear manufacturing. There is some specific work with regards to the application of these more advanced techniques to CURVIC coupling inspection, but the current body of research stops short of inspecting coupling contact pattern. Practices for inspection of more common gear forms, such as spur and hypoid gears, using advanced methods are reviewed as a foundation for extrapolation to the CURVIC coupling.

Having reviewed current practices and applications of both CURVIC coupling inspection and advanced metrology solutions, a method of digital analysis is proposed and carried out in addition to traditional contact pattern analysis. Both of these investigations were carried out on sample CURVIC coupling test pieces that were designed following recommended practices as described by Gleason, the organization responsible for the coupling's development. The steps of test piece design and manufacture are covered to address limitations that were imposed on this investigation due to available resources.

Lastly, a comparison of the results obtained by the traditional transfer method for inspecting contact pattern and the employed method of using a CMM for digital analysis is performed. These results are explained and suggestions for future work are proposed.

Chapter 2: Literary Review

2.1 Fixed CURVIC Coupling Geometry

CURVIC couplings are primarily made as one of three different types: the Fixed Coupling, the Semi-Universal coupling, and the Releasing Coupling [5]. The fixed Curvic coupling is also sometimes referred to as a Permanent CURVIC Coupling due to its use in applications where the components being coupled are constantly attached and viewed as a single operating unit. This allows for the design of the coupling to be optimized for accurate alignment, precision centering, and positive drive.

The teeth of a fixed CURVIC coupling are cut, cut and ground, or ground to a constant depth across the face of a solid component. One member of the coupling is made with convex, or "barrel-shaped", teeth, and its mate is made with concave, or "hour-glass-shaped", teeth as illustrated in Figure 1:

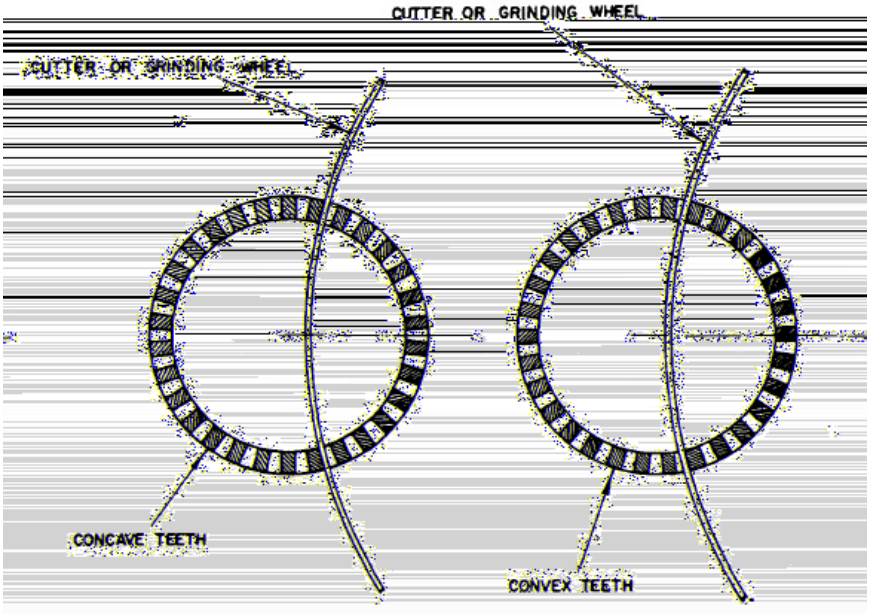

FIGURE 1. CONVEX AND CONCAVE MEMBERS, ADOPTED FROM [2]

The radius of the cutter or grinding wheel being used, the size of the part, and the number of teeth are all interdependent and follow the basic relationship below [2]:

n_x = number of half pitches included between two engagements of grinding wheel.

N = number of teeth in CURVIC coupling.

r = radius of grinding wheel.

A = mean radius of CURVIC Coupling.

then $\beta = (90^\circ X\ n_x) / N$

and $r = A \tan B$

These calculations are performed in conjunction with others to determine the size of coupling necessary to handle a given amount of torque. With a size and tooth count established additional "Standard Tooth Proportions" are used to define elements such as whole depth, addendum, and dedendum based on recommended diametrical pitch values. The recommendations defined by Gleason are as follows [2, 3]:

$P_d = N/D$ $\qquad$ $c_t = .090/P_d$

$h_t = .880/P_d$ $\qquad$ $a = (h_t - c)/2$

$c = .100/P_d$ $\qquad$ $b = h_t - a$

P_d = Diametrical pitch at the outside diameter

D = coupling outside diameter

c = clearance

c_t = chamfer height

h_t = whole depth

a = addendum

b = dedendum

It has been found that the most practical pressure angle is 30° for fixed CURVIC Couplings, however angles as low as 10° or as high as 40° can be used [2]. Regardless of coupling pressure angle, the resulting tooth surface can be geometrically defined by mathematical equations of a cone [8]. Figure 2 displays the location of previously defined dimensions:

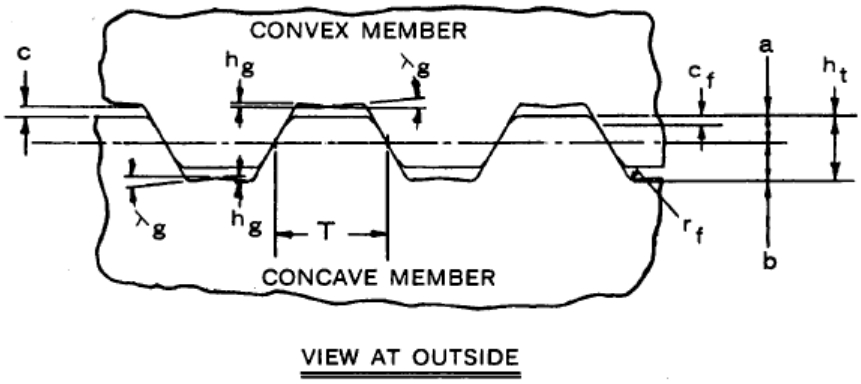

FIGURE 2. VIEW OF MATING MEMBERS, ADOPTED FROM [2]

2.2 CURVIC Coupling Inspection

The nature of many components featuring CURVIC couplings is to be interchangeable and easily replaced while the assembly maintains its critical features. To provide this capability various key features of the coupling must be controlled in such a manner as to insure compliance of the assembly regardless of when individual components were manufactured. Certain discrete features that define the individual tooth such as size of fillet radii and chamfers as well as the whole depth of the tooth profile can be inspected with traditional gages and optical comparators. Figure 3 shows an optical comparator with inspection template overlay being used to inspect the general profile of the tooth.

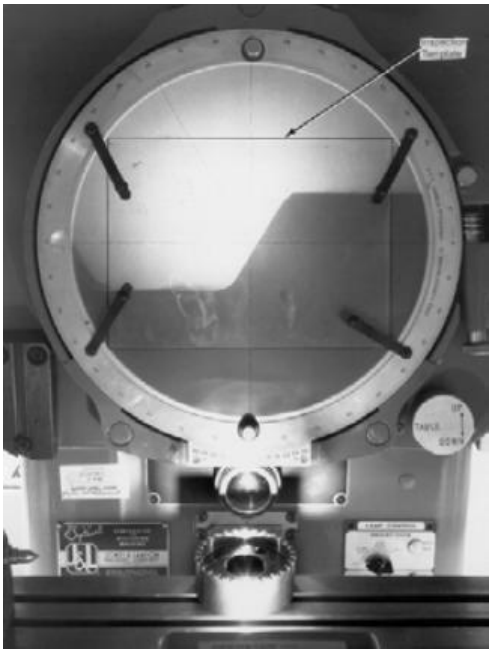

FIGURE 3. TOOTH FORM INSPECTION ON OPTICAL COMPARATOR, ADOPTED FROM [4]

Many other attributes relating to the couplings ability to conform to specification within an assembly are inspected with the use of a control, or “master”, coupling. The master coupling is used to provide a single reference piece for which production couplings can be fitted and behaviors within the finished assembly can be inferred. Characteristics requiring the use of a master coupling for inspection include: stacking distance, runout inspection, alignment inspection, and tooth contact pattern inspection [4]. Figure 4 shows the use of two master couplings to on either side of the produced double ended part being used on a rotary table to measure both the axial and radial runout.

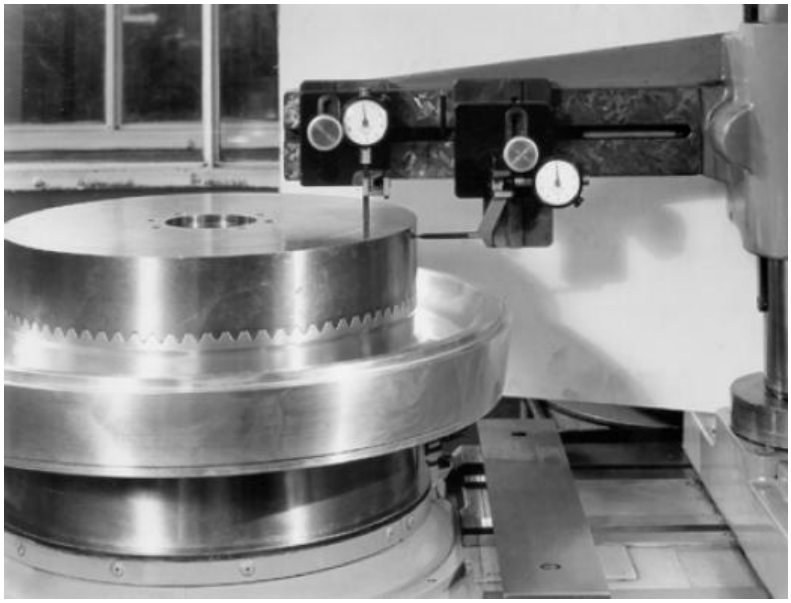

FIGURE 4. INSPECTION OF AXIAL AND RADIAL RUNOUT OF DOUBLE ENDED PART, ADOPTED FROM [4]

The previously discussed features or attributes of the CURVIC coupling provide discrete and quantifiable results when inspected. One critical area of inspection related to the coupling's ability to perform as designed that is not easily quantified, but rather interpreted, is the contact pattern across the teeth of the gear that results when two elements are coupled together. The process of determining this contact pattern requires multiple steps, some of which are subjective and have the potential to vary from operator to operator, more so than typically seen between operators measuring a standard dimension with a set of micrometers.

The basic procedure that Gleason recommends for determining tooth contact pattern is as follows [4]:

1. Using a two-brush method apply a thin coat of marking compound to the production part and use the second brush to smooth and remove away excess compound.
2. Utilizing the same two-brush method apply a thin coat of marking compound of contrasting color to the master coupling.
3. Blow off both couplings with compressed air to remove any foreign particulate.
4. Carefully mate the two couplings by placing one on top of the other.
5. Lightly tap directly over the teeth around the circumference of the coupling with a soft mallet to seat the two and transfer marking compound.
6. Carefully separate the coupling.
7. Inspect transfer of marking compound to produced part for satisfactory contact.

Figure 5 shows a section of teeth that have been subjected to the transfer of marking compound from a master coupling. The areas of contact can be seen as dark bands across the face of each tooth.

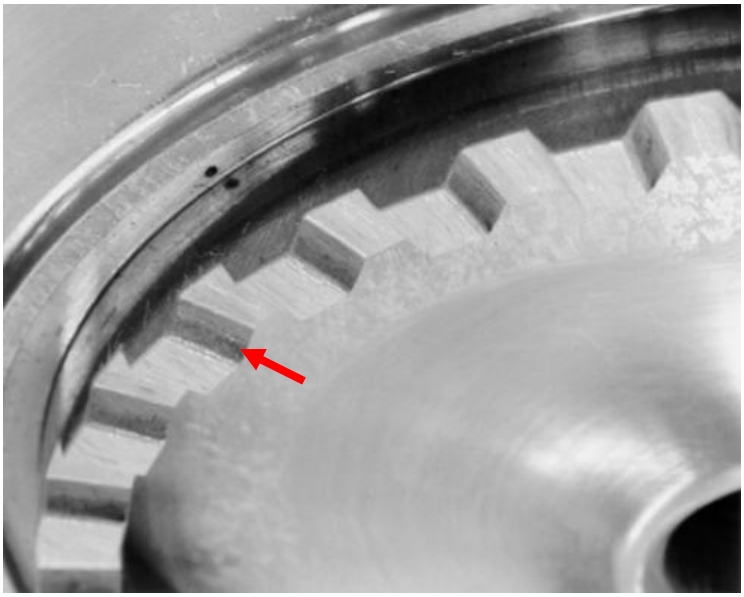

FIGURE 5. MARKING COMPOUND TRANSFER, ADOPTED FROM [4]

Having carefully completed the above steps and being left with a coupling displaying areas of contact the operator then determines if satisfactory contact has been made between the production and master coupling. If determined to be satisfactory it is inferred the same contact characteristics will be seen with other couplings produced in the shape of the master. Figure 6 provides examples of both acceptable and unacceptable transfer patterns.

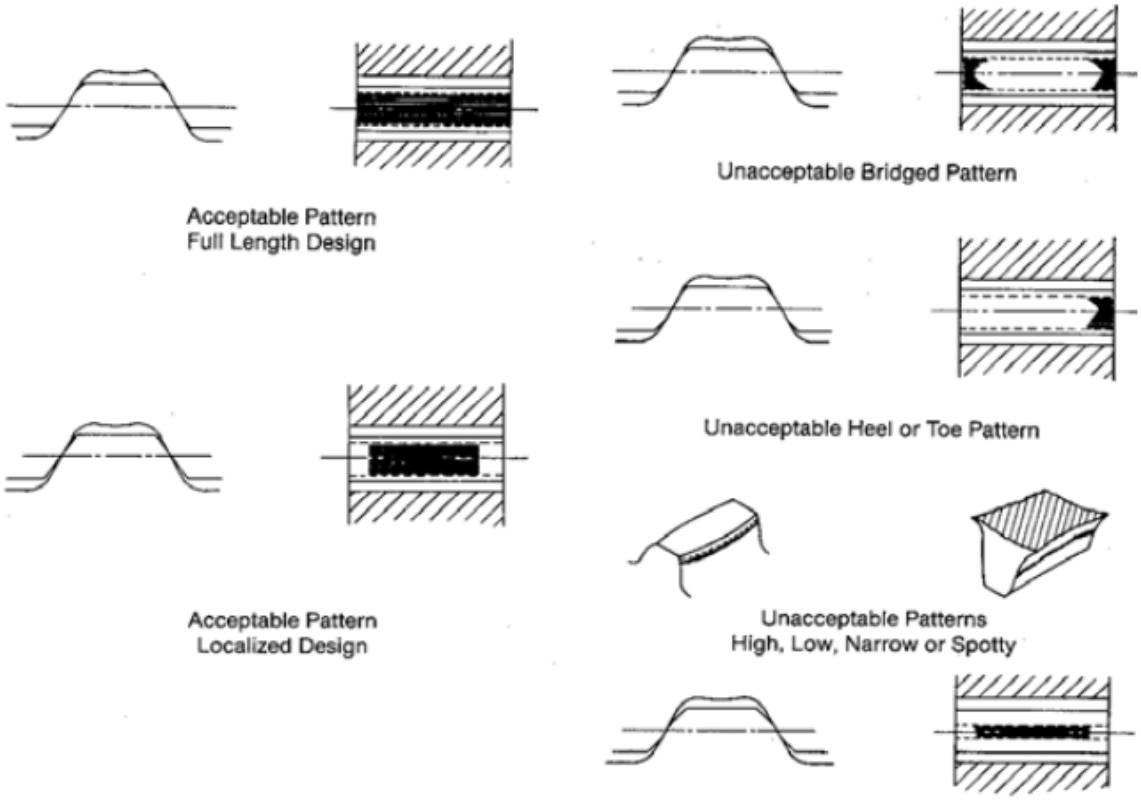

FIGURE 6. TOOTH CONTACT PATTERNS, ADOPTED FROM [4]

In addition to looking at the contact pattern seen on individual teeth, engineering design specifications may dictate how many teeth must have acceptable contact patterns as well as the location of those teeth with respect to the entire profile. This pattern is observed in process, and if necessary machine settings are adjusted to improve contact pattern results.

2.3 Metrology of Complex Surfaces

The emergence of advanced design and manufacturing capabilities has resulted in a need to accurately define and control surfaces of complex shape. Components containing surfaces of this nature can be found in many of today's prominent industries such as aerospace, automotive, and medical device manufacturing. Traditionally, components are measured by direct comparison using a master gage or template to check the amount of

deviation between the produced part and the ideal shape as defined by the master gage. This method has some notable shortcomings, primarily: accuracy, speed, and the need to have dedicated equipment [15]. The use of master gages in measuring the contact pattern between mating CURVIC couplings is no exception.

Many modern techniques of measuring complex surfaces now exist that are capable of generating dimensional data for analysis. A CMM, optical scanner, laser tracker, or other method is used to collect and record the location of various points over an area of the surface being measured.

An evaluation of some measurement techniques with relation to their performance in several applications is shown in Table 1.

TABLE 1. EVALUATION OF MEASURMENT TECHNIQUES, ADOPTED FROM [15]

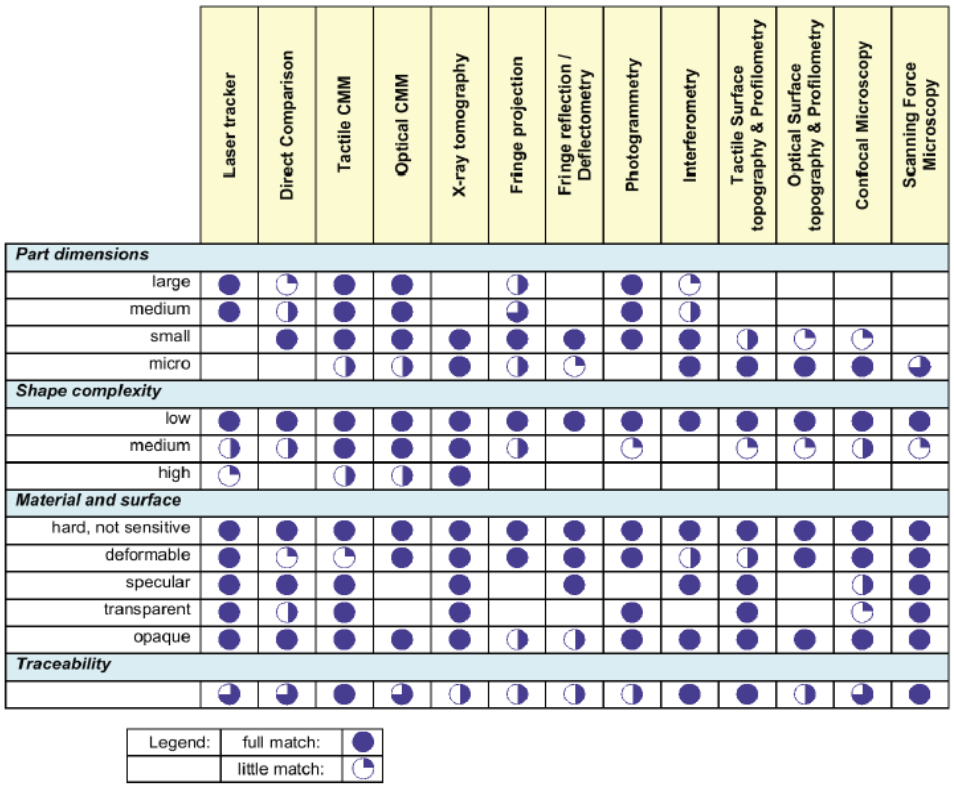

Multiple strategies for the sampling of data points also exist. The most basic of these strategies is a uniform distribution of points with a constant distance between points across the surface. The result of applying these techniques is a collection of points in space that are commonly referred to as a "point cloud". Following filtering and alignment of the point cloud to the nominal geometric data an evaluation of the measurements can be performed.

Evaluation is typically done using computer programs that display a map of deviation from nominal dimensions. The model is shown with a color gradient applied across the surface with different colors associated with varying degrees of discrepancy from nominal. Figure 7 shows an application of this method.

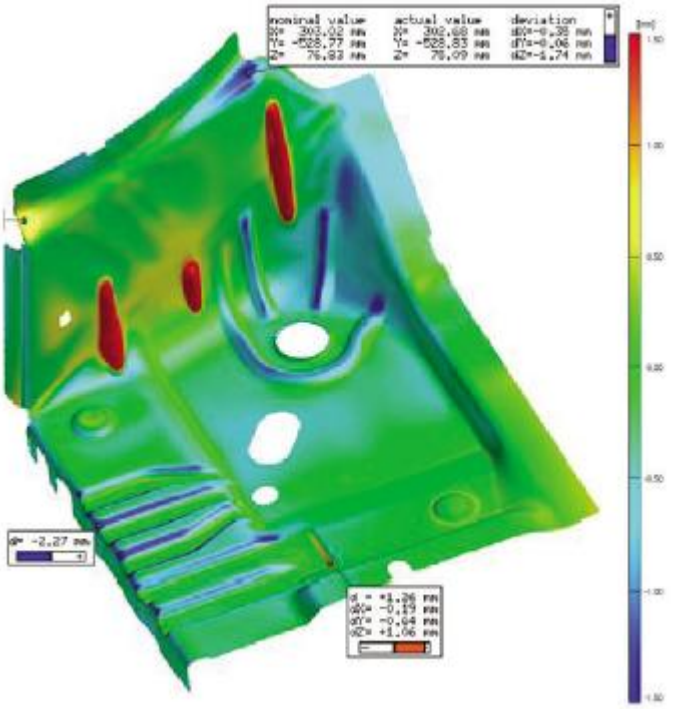

FIGURE 7. MAP OF DEVIATIONS, ADOPTED FROM [15]

Each method previously discussed is capable of inducing errors of varying degree into the measurement sample. An additional source of error that should be taken into account is error induced by the software being used, or the transfer of collected data from one format to another.

2.4 Use of CMMs in Gear Metrology

The versatility of CMMs and their ability to inspect complex features led to the adoption of this technology for inspection by gear manufacturers soon after its introduction. There was initially some gap between the capabilities between CMMs and specialized gear measuring instruments (GMI) however, with advancement in technologies and options available for CMMs the gap has closed [7].

Originally the use of CMMs for measurement of gear profiles was done in a way to mimic the traditional methods of the time. This results in a simplified expression of the gear surfaces that can be defined in two dimensions and requires measurements to be taken from predetermined points of interest. As a result of the limitations of this approach a three-dimensional representation of gear flanks from CMM measurements was developed [11].

A three-dimensional representation of the gear being measured is created by the sampling of multiple points without restriction to either the transverse plane or pitch cylinder. A surface of best fit is then generated from the point cloud data to prove a three-dimensional representation of the entire surface in question. Figure 8 provides and illustration of this method.

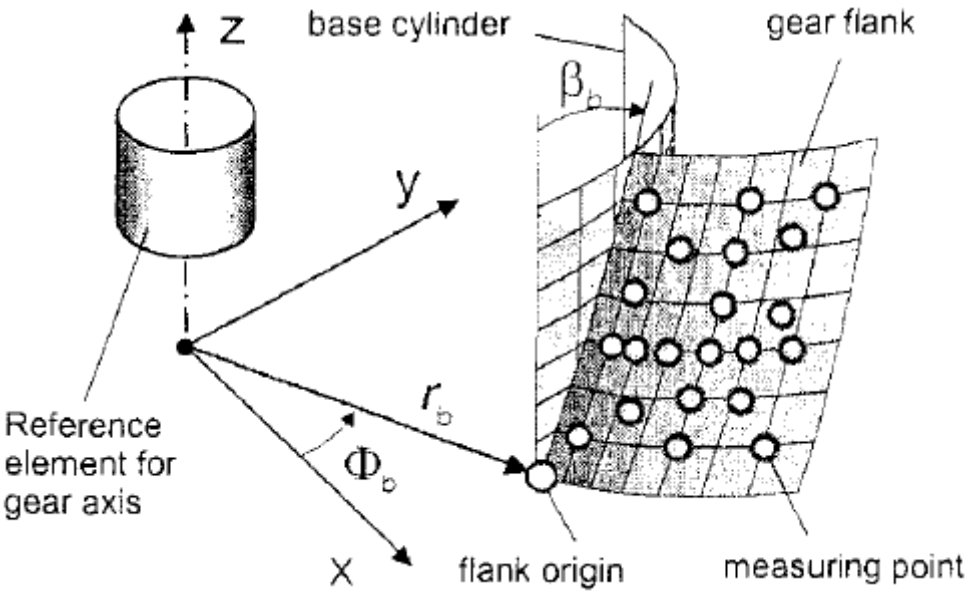

FIGURE 8. GEAR FLANK REPRESENTATION FROM POINT CLOUD, ADOPTED FROM [11]

The use of CMMs in this capacity is not without concern. The primary concern is the accuracy of the machine being used to collect measurement data. The market for CMMs is such that the promise of more accurate capabilities is accompanied by a substantial increase in price. Research with regards to the amount of necessary performance for the measurement of CURVIC couplings by CMM has resulted in findings that "low-cost" machines are capable of providing acceptable results comparable to those obtained my CMMs with better specifications [13]. Another area of concern is the amount of time required for inspection by this method. This is due to the use of a 3D stylus to sample points, one at a time, from the surface. Consideration must be taken with respect to how many points are necessary to accurately represent the surfaces being measured. The sampling interval should then be large enough to require only the minimum amount of

points necessary, but small enough to maintain an accurate representation of the surface [12].

2.5 Estimating Tooth Contact Pattern

There currently exists a method for estimating the contact pattern of bevel and hypoid gears. This method is known as Tooth Contact Analysis, or TCA, and could be expanded for use with CURVIC couplings.

TCA is a mathematical tool that uses a computer to determine the contact and motion seen between a pair of hypoid or bevel gears [6]. This method of analysis was developed to reduce the amount of trial and error associated with attempting to produce desirable contact patterns with new gear designs on test machines. With gear profiles being determined by machine settings and cutter shapes these parameters can be input into the computer along with operating parameters of the gear set to develop the estimation of contact and motion. Success has also been had through tooth surface approximation and solving for areas of tangency [1]. This is accomplished by noting areas where the difference between two functions representing the surfaces being investigated is equal to zero [9, 10].

One finding through the development of TCA is that the gears being evaluated can be said to be in contact when there is a difference of less than .00025” between the surfaces of the gears [6]. This value was extrapolated from gear testing using marking compound where it was noticed that, under light load, transfer of compound would occur when this difference between surfaces was less than .00025”.

Chapter 3: Methodology

3.1 Roadmap of Methodology

The following image is to serve as a guide for the reader to present the flow of this investigation, as well as the structure of this section and results.

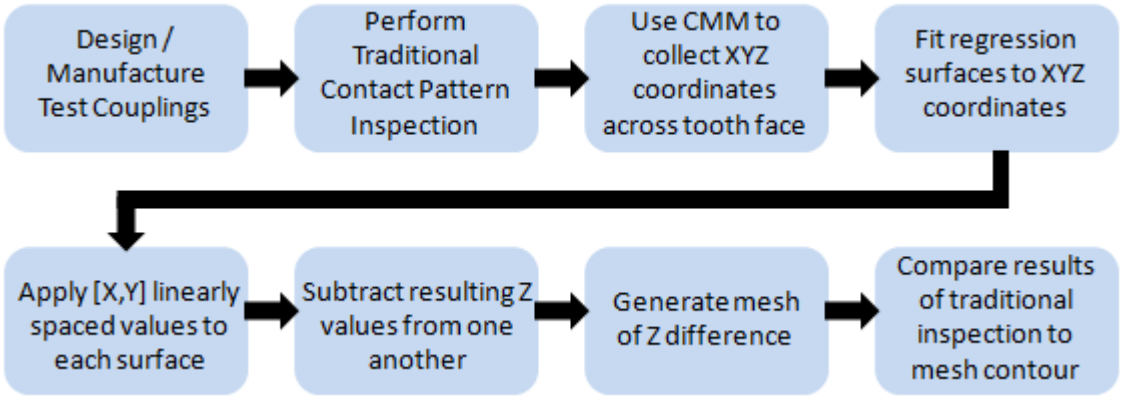

FIGURE 9: ROADMAP OF METHODOLOGY

3.2 Test Coupling Design and Manufacture

3.2.1 Design Considerations and Solid Modeling

Due to the lack of access to a set of mating CURVIC couplings it was decided the best course of action would be to design and manufacture a set using Gleason's dimensional design specifications. Other notable design and manufacture limitations include type of material, size of coupling, tooling used, and method of manufacture. Workarounds to these limitations were employed with consideration given at each step to ensure suitability for the purpose of this investigation.

The size of material available for use was a primary determining factor for the design of the coupling. Aluminum was chosen as the preferred type of material due primarily to its good machinability, while maintaining an appropriate level of strength and dimensional fortitude for the purpose of this research. A 3.5" round stick of 2024 aluminum alloy was found and determined to be the best option available. An outside diameter of 3.250", to allow for the turning of a machined surface in the axial direction, provided the outside diameter component of future calculations.

In addition to the outside diameter of the coupling, the number of teeth and face width of the teeth were the other factors that needed to be decided for the final coupling to be fully defined. A face width of .375" and tooth count of 12 was determined to provide teeth of adequate size and number for future stylus probing with a CMM and maintain conformance to Gleason's specified design limitations and suggestions. Having defined these three critical values, Gleason's recommended equations for fixed CURVIC couplings, presented earlier in this paper, were employed to fully define the test couplings and provide the foundation for development of a solid-model. Tables 2 and 3 show the independent and calculated values.

TABLE 2. INDEPENDENT VALUES USED FOR TEST COUPLING DESIGN.

Independent Values		
Number of Teeth	N	12
Outside Diameter	D	3.25
Face Width	F	0.375

TABLE 3. CALCULATED VALUES USED FOR TEST COUPLING DESIGN.

Calculated Values

Mean Radius	A	1.4375	"Grinding Wheel Radius"	r	3.4704
Diametrical Pitch	P_d	3.6923	Chamfer Height	c_t	0.0244
Whole Depth	h_t	0.2383	Addendum	a	0.1056
Clearance	c	0.0271	Dedendum	b	0.1327

Both concave and convex test couplings were modeled in three-dimensions using the same values. Revolved cutouts with a 30 degree angled component, to establish the proper pressure angle, were utilized to mimic the material removal process seen in production. The difference in concave and convex couplings was established by whether material was "removed" towards the inside or outside of the revolved 30 degree member. In addition to the necessary geometry for coupling purposes, a circular pocket of .675" was also incorporated and offset from center to provide a rotational reference point. Figure 10 is a composite image of both couplings individually and coupled.

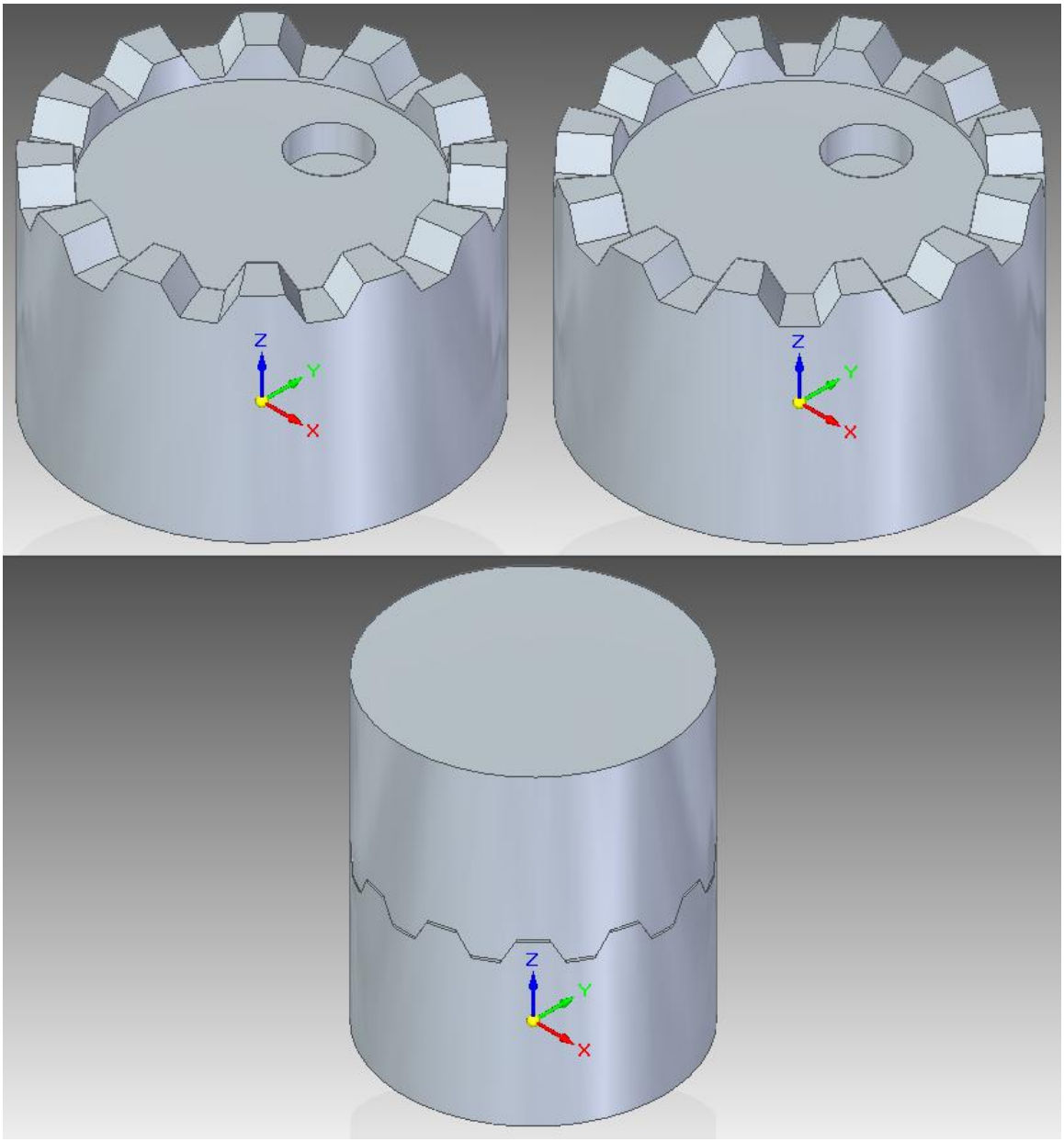

FIGURE 10. COMPOSITE IMAGE OF CONCAVE, CONVEX, AND JOINED COUPLINGS

3.2.2 Tool Selection and CAM Programming

The solid models shown above were imported into a CAM package for generation of the machine G-Code to be later executed on a 3-axis milling machine. It was at this point that tool size was determined to provide the most rigid setup that could still perform within

the small confines between teeth. Table 4 lists the cutters selected for milling of the teeth and pocket geometry.

TABLE 4. TOOLS USED FOR MILLING OPERATIONS.

Milling Tools

3"	5-Tooth	Face Mill	Carbide Insert
.375"	2-Flute	Flat Endmill	HSS
.375"	2-Flute	60 Degree Chamfer Tool	Solid Carbide
.125"	2-Flute	Flat Endmill	Solid Carbide

Tool paths for machining the surface profile were generated at an off machine computer workstation in the following order:

1. Standard Pocket (Center Pocket): .375” Flat Endmill - .150” DOC / .050” Finish Step - 75% Step Over Parallel Spiral / .005” Finish Pass
2. Standard Pocket (Locating Pocket): .375” Flat Endmill - .150” DOC / .050” Finish Step - 75% Step Over Parallel Spiral / .005” Finish Pass
3. 2D Contour (Locating Pocket): .125” Flat Endmill - .100 DOC
4. Surface Rough Pocket (Tooth Profile Rough): .125” Flat Endmill – 0” left on Drive Surfaces / .050” Max Step - 55% Step Over Parallel Spiral / .005” Finish Pass
5. Transform Surface Rough Pocket x 12 times
6. 2D Contour (Tooth Face): 60 Degree Chamfer Mill - Center Tool on Curve
7. Transform 2D Contour x 12 times

These tool paths were created for execution on slugs of 2024 Al previously turned and faced to size. The first and second paths establish the inside face of the teeth as well as the locating pocket. The 2D Contour pass with the .125” endmill used the locating pocket’s known final diameter as a reference to ensure proper diameter compensation is made within the controller due to difficulty of directly measuring the following tooth roughing operations with conventional methods while the work piece is in the machine. Having set proper compensation on the .125” endmill it is used for roughing the space between each of the twelve teeth with a Surface Rough Pocket operation that is transformed around the z-axis with 30 degrees of separation between each copy. The final toolpath, 2D Contour, establishes the 30 degree pressure angle of the teeth using a 60 degree chamfer mill programmed for the tip to follow the curve at the base of the tooth face. Similar to the Surface Rough Pocket toolpath, this toolpath is also transformed about the z-axis with 30 degrees of separation between each copy.

This process was the same for both concave and convex couplings.

3.2.3 Material Removal

The machining process started with the cutting of two pieces roughly 2.5” long from the bar of 2024 Al. These pieces were each chucked into a lathe and then faced on one end and turned to the final diameter of 3.250” for a length of 2.1”. One end was left rough to later be faced while in the mill.

Before milling operations could commence a set of aluminum soft jaws for a 6” machinist’s vise were fabricated. Each jaw featured profiles consistent with the outside

surface of the work piece and a shoulder for the bottom of the work piece to contact roughly .5” below the top surface of the jaws.

Tooling was loaded in solid holders with exception of the .125” endmill which was put into an ER collet holder. The tools were then loaded and tool height offset set off the top of a 1-2-3 block set on the back of the 6” vise. An additional .025” was added to the length of the 60 degree chamfer tool in the controller to avoid removing excess material due to the tip not coming to an exact point as expected by the CAM program. Home location G54 Z0 was then sent as the distance from the top of the 1-2-3 block to the ledge in the soft jaw where the bottom of the work piece will contact. One of the turned work pieces was loaded into the vise and home location G54 X0 Y0 was found by sweeping the outside diameter with a dial indicator.

Code required for the facing of the work piece to size was written at the controller and made use of the 3” face mill. Once the work piece was verified to be 2.000” inches in height the program previously described was executed. Minor adjustments for feed and speed were made on the fly and were the only adjustments required until the running of the 60 degree chamfer tool. The 60 degree chamfer tool still required its tool height to be precisely specified. It was run multiple times and lowered a small amount after each pass until the striations left by the .125” endmill were no longer visible. It was concluded that this would be the proper tool height for the chamfer mill to run at since 0” was left on drive surfaces when programming the .125” endmill.

This process was repeated for the remaining coupling using the same tool offset values and adjusted feed and speed.

With machining operations complete on both concave and convex couplings they were deburred by hand, with care taken to avoid scoring the tooth face.

3.3 Traditional Contact Pattern Inspection

The contact pattern seen between the couplings machined for this investigation was carried out in a manner similar to the one Gleason recommends. The difference being that only one coupling was coated with marking compound and transfer of that single color was observed. The light color of machined aluminum allowed for the single color transfer to still be easily seen. It should be noted that in industry this comparison would be carried out between one produced coupling and one master coupling. The following figure shows the coated convex coupling and the transfer to the bare concave coupling.

FIGURE 11. COMPOSITE IMAGE SHOWING TRANSFER OF COLOR

Repeatability was achieved after overcoming a learning curve with regards to the proper application of marking compound. The following table describes the pattern seen from two independent trials.

TABLE 5. TRANSFER PATTERNS FROM TWO TRIALS

Intersection	Trial A	Trial B
1	Slight transfer towards inside edge	Significant transfer across center
2	Full Transfer	Full Transfer
3	No Transfer	No Transfer
4	Significant transfer across center	Slight transfer towards outside edge
5	Slight transfer across center	Significant transfer across center
6	No Transfer	No Transfer
7	Full Transfer	Full Transfer
8	No Transfer	No Transfer
9	Full Transfer	Full Transfer
10	Significant transfer across center	Significant transfer across center
11	Significant transfer across center	Significant transfer across center
12	Full Transfer	Full Transfer
13	Significant transfer across center	Significant transfer across center
14	Full Transfer	Full Transfer
15	Slight transfer across center	Slight transfer across middle
16	Significant transfer across center	Full Transfer
17	Slight transfer across center	Significant transfer across center
18	No Transfer	Slight transfer across center
19	Full Transfer	Full Transfer
20	No Transfer	Slight transfer across center
21	Full Transfer	Full Transfer
22	Significant transfer across center	Significant transfer across center
23	No Transfer	No Transfer
24	Full Transfer	Full Transfer

The possibility for significant variation with this method of analysis becomes even more apparent while performing this test. What is a thin film? What is slight transfer? Each of the two trials was performed in the same rotational orientation where the couplings were placed into contact with each other in such a fashion that the same surfaces that are in contact during Trial A are placed back into contact for Trial B.

3.4 CMM Based Contact Pattern Inspection

The CMM used to collect data for analysis was a shop-floor type machine in a small room that is kept air conditioned. Both manufactured couplings were inspected on the same machine under the same conditions. Programs were developed to capture 25 points across the face of each tooth with the origin specified to be the same as that which was used when modeled. Each coupling was measured twice and the results averaged to create the positional data used for analysis. This data was then classified as 24 separate sets of data per coupling, each with X, Y, and Z positional components, and corresponding to a single specific tooth face.

Due to both couplings being measured with the teeth in the +Z direction some translation of data was necessary to account for the inversion of one coupling when corresponding tooth faces are placed in contact with each other. This was accomplished by mirroring across the X-axis as well as the CURVIC pitch plane. The data collected for the concave and convex couplings should now, in theory, represent the same surface if complete contact is considered.

The data was then imported into a computerized mathematical analysis package for the computation of regressed surfaces. After applying multiple methods of interpretation it was found that a linear method resulted in the best fit with SSE values in the range of e-32. The following two images show the interpolated surfaces for the concave coupling and convex coupling, along with relevant surface fitting information, at what is defined as Intersection 1.

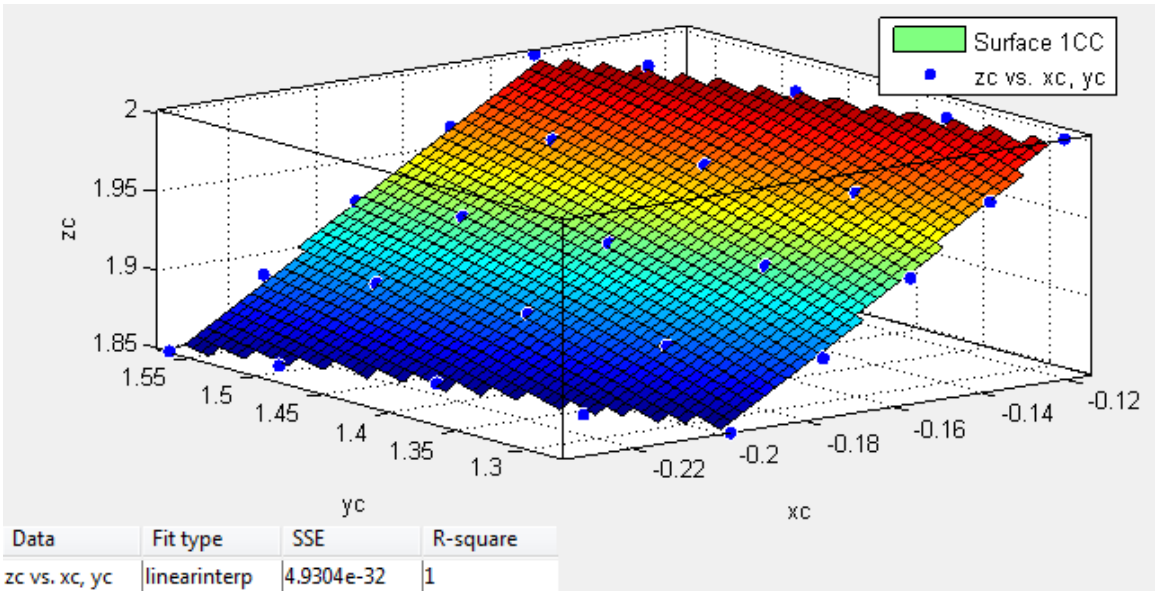

FIGURE 12. INTERPOLATED SURFACE OF CONCAVE COUPLING AT INTERSECTION 1

Linear interpolant:
f(x,y) = piecewise linear surface computed from p
where x is normalized by mean -0.1755 and std 0.03374
and where y is normalized by mean 1.426 and std 0.1064
Coefficients:
p = coefficient structure

Goodness of fit:
SSE: 4.93e-032
R-square: 1

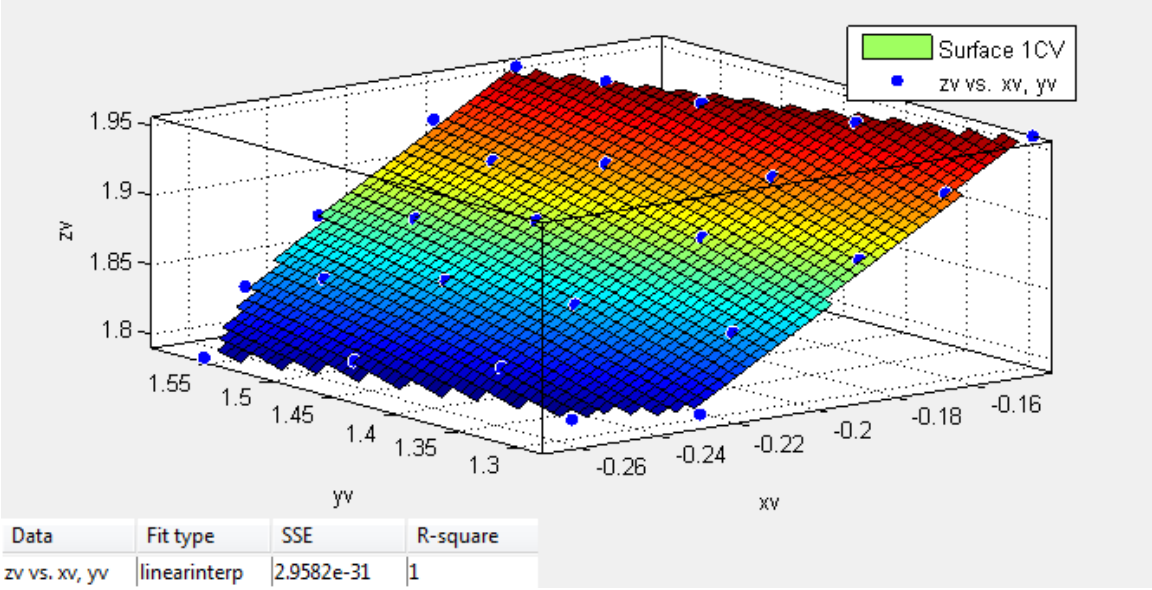

FIGURE 13. INTERPOLATED SURFACE OF CONVEX COUPLING AT INTERSECTION 1

Linear interpolant:
f(x,y) = piecewise linear surface computed from p
where x is normalized by mean -0.2073 and std 0.0343
and where y is normalized by mean 1.452 and std 0.1056
Coefficients:
p = coefficient structure

Goodness of fit:
SSE: 2.958e-031
R-square: 1

To find the distance between two surfaces a 100x100 matrix of linearly spaced X,Y values was created within the boundary of surface overlap. Z-values from the fitted surface representing the convex surface were then subtracted from the Z-values of the fitted surface representing the concave surface. A mesh of the difference was then created across the same 100x100 matrix of linearly spaced X,Y-values in an attempt to show likely areas of contact. This contact would be expected to take place at the lowest values. As with the traditional analysis, rotational variation was limited and only one orientation

was evaluated. The orientation that was evaluated by CMM being the same orientation evaluated during the traditional analysis. The mesh of the difference in Z-values for Intersection 1 is typical of the other 23 intersections and shown in the figure below.

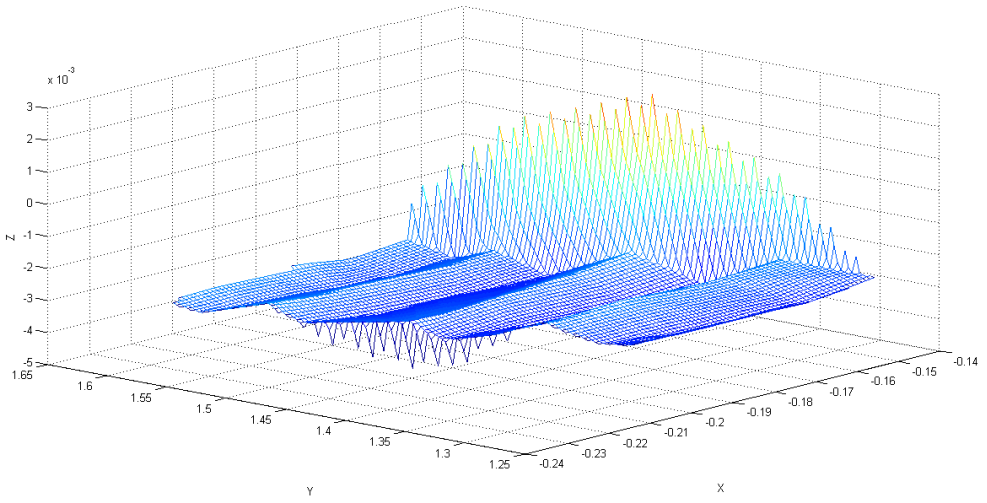

FIGURE 14. MESH OF DIFFERENCE IN Z-VALUES BETWEEN INTERPOLATED SURFACES

Both areas of extreme values at maximum and minimum X are due to sampling of data crossing into the rounded areas towards the top of the tooth face. One area appears negative due to the translation of data, however both are indicative of a growing distance between surfaces. An interesting wave pattern appears across the majority of the mesh. If this mesh is representative of contact, one would expect to see a series of stripes running from the root to the top of the tooth. Considering the method of manufacture as well as the method of point location sampling with the CMM, this pattern is believed to have been imparted by the surface fitting process. To test this hypothesis a different form surface fitting was used, in this case a polynomial with 2 degrees in both X and Y. For surface 1CC the resulting equation of fit becomes:

Linear model Poly22:
f(x,y) = p00 + p10*x + p01*y + p20*x^2 + p11*x*y + p02*y^2
Coefficients (with 95% confidence bounds):
p00 = 1.399 (1.392, 1.406)
p10 = 1.615 (1.603, 1.628)
p01 = 0.9242 (0.9146, 0.9338)
p20 = 0.04446 (0.008844, 0.08008)
p11 = 0.07717 (0.06483, 0.0895)
p02 = -0.2401 (-0.2435, -0.2366)

Goodness of fit:
SSE: 8.554e-008
R-square: 1
Adjusted R-square: 1
RMSE: 6.71e-005

Surface 1CV sees similar results with a polynomial fit described as follows:

Linear model Poly22:
f(x,y) = p00 + p10*x + p01*y + p20*x^2 + p11*x*y + p02*y^2
Coefficients (with 95% confidence bounds):
p00 = 1.396 (1.387, 1.405)
p10 = 1.616 (1.6, 1.632)
p01 = 0.9334 (0.9209, 0.9459)
p20 = -0.1176 (-0.1609, -0.07439)
p11 = 0.0345 (0.02004, 0.04895)
p02 = -0.2464 (-0.2508, -0.2421)

Goodness of fit:
SSE: 1.462e-007
R-square: 1
Adjusted R-square: 1
RMSE: 8.772e-005

Again, the difference between these two fits was analyzed and produced the mesh seen in Figure 14 that shows the interaction at Intersection 1 and is typical of the other 23 areas of interaction.

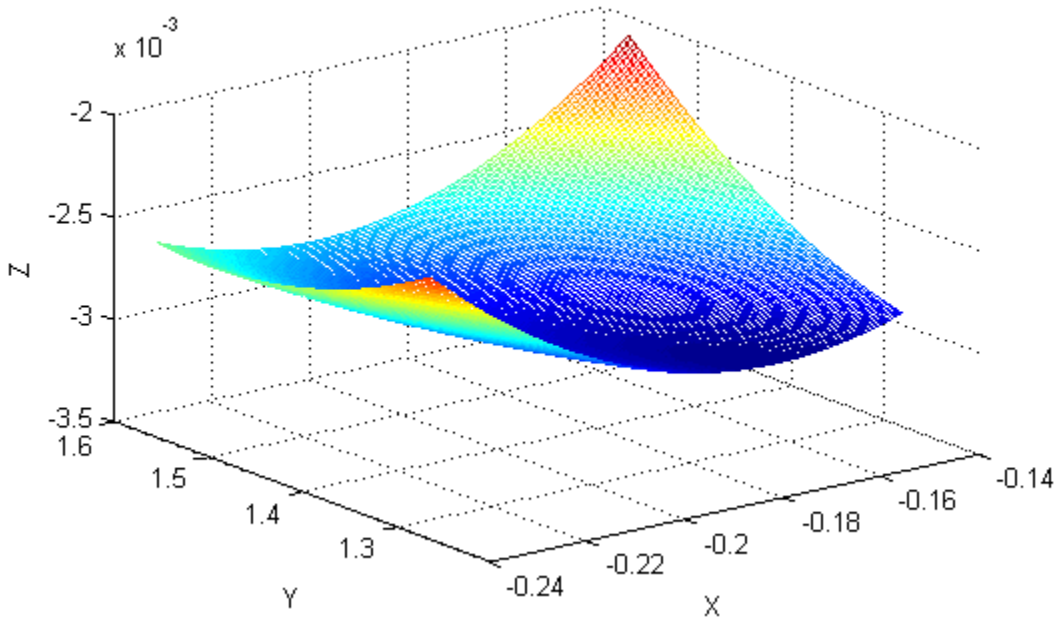

FIGURE 15. MESH OF DIFFERENCE IN POLYNOMIAL FIT SURFACES

The resulting mesh of difference using the polynomial fit surfaces produces a much smoother mesh that displays similar characteristics as the previously documented linear interpolated result in terms of absolute position. Similarly, the likely areas of contact taking place in the lowest lying regions.

Chapter 4: Results

4.1 Comparison of Analysis

It is readily apparent that the results seen from the application of the current industry standard for CURVIC coupling contact pattern inspection were not recreated using the methods described in Section 3.3. This, however, does not mean that there is not some type of relationship or useful information that can be gleaned from the data collected.

Using the mesh of differences, an average Z-value and magnitude of the depicted waveform were estimated for each intersection. These values were then compiled with the descriptions of contact from the traditional analysis method and sorted to see if any relationships existed.

Sorting by average Z-value does provide an apparent correlation between the amount of transfer seen and the average Z-value: Smaller Z-values corresponding to more transfer and larger values being associated with little or no transfer. This is to be expected as the smallest Z-value could be considered zero distance between surfaces with the gap between them growing as Z increases. It is less apparent whether the magnitude of the waveform seen with the linear fit, or the range of lowest values seen with the polynomial fit, has any relation to the amount of transfer seen. It is important to note that the actual value of Z is somewhat arbitrary and derived from the value used as the location of the CURVIC pitch plane during transformation, and that it is the range of values that describes the distance from a nominal point of contact which takes place at the lowest value Z.

To better illustrate any correlation, the amount of contact observed from the physical transfer was given a numerical value between one and four. One being associated with no transfer and four being associated with full transfer. The following two figures show both the average Z-values as well as the range values plotted in this manner. Each dot represents an area of interaction between concave and convex couplings.

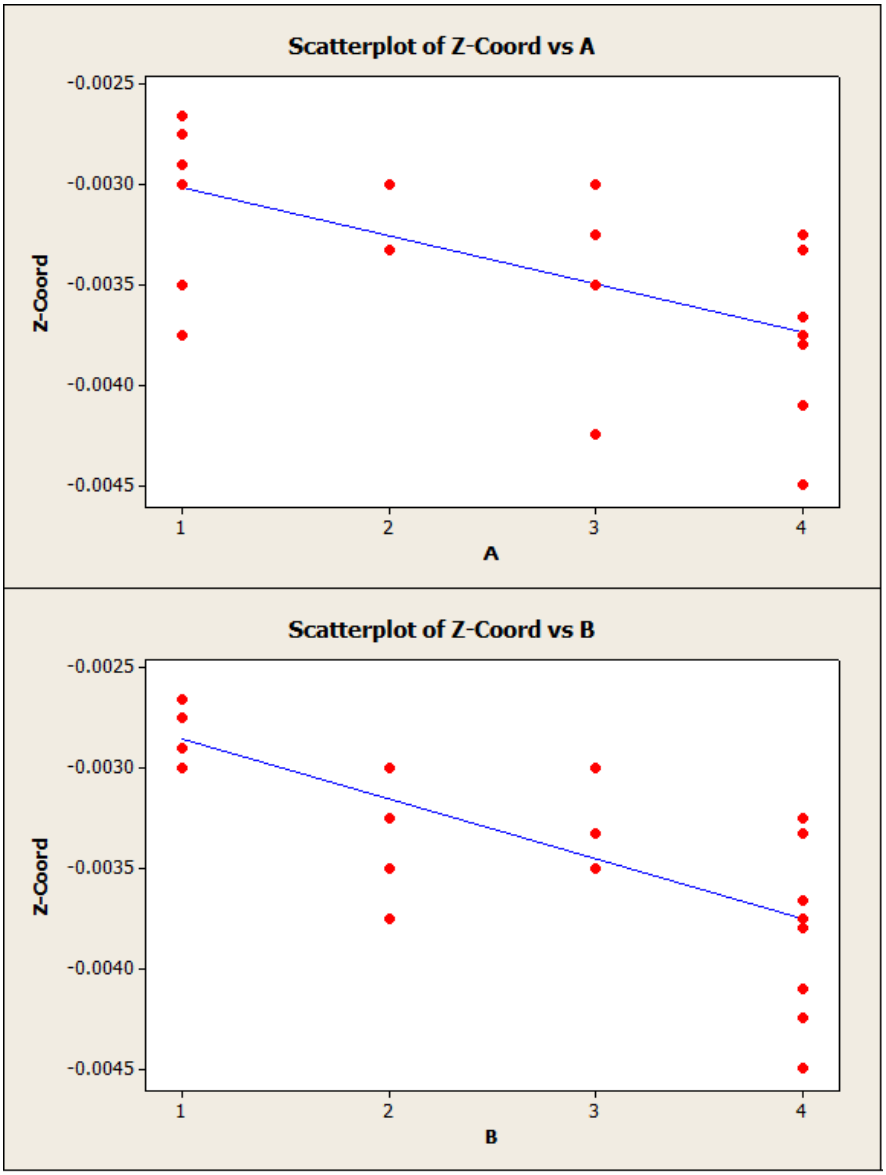

FIGURE 16. PLOTS OF CONTACT VS. AVERAGE Z-COORDINATE VALUES

While the previous plots do show some correlation, the associated R-sq values of the regression lines are rather low at 37.8% for Trial A and 49.5% for Trial B. This is likely due in large part to only having four degrees of transfer classification.

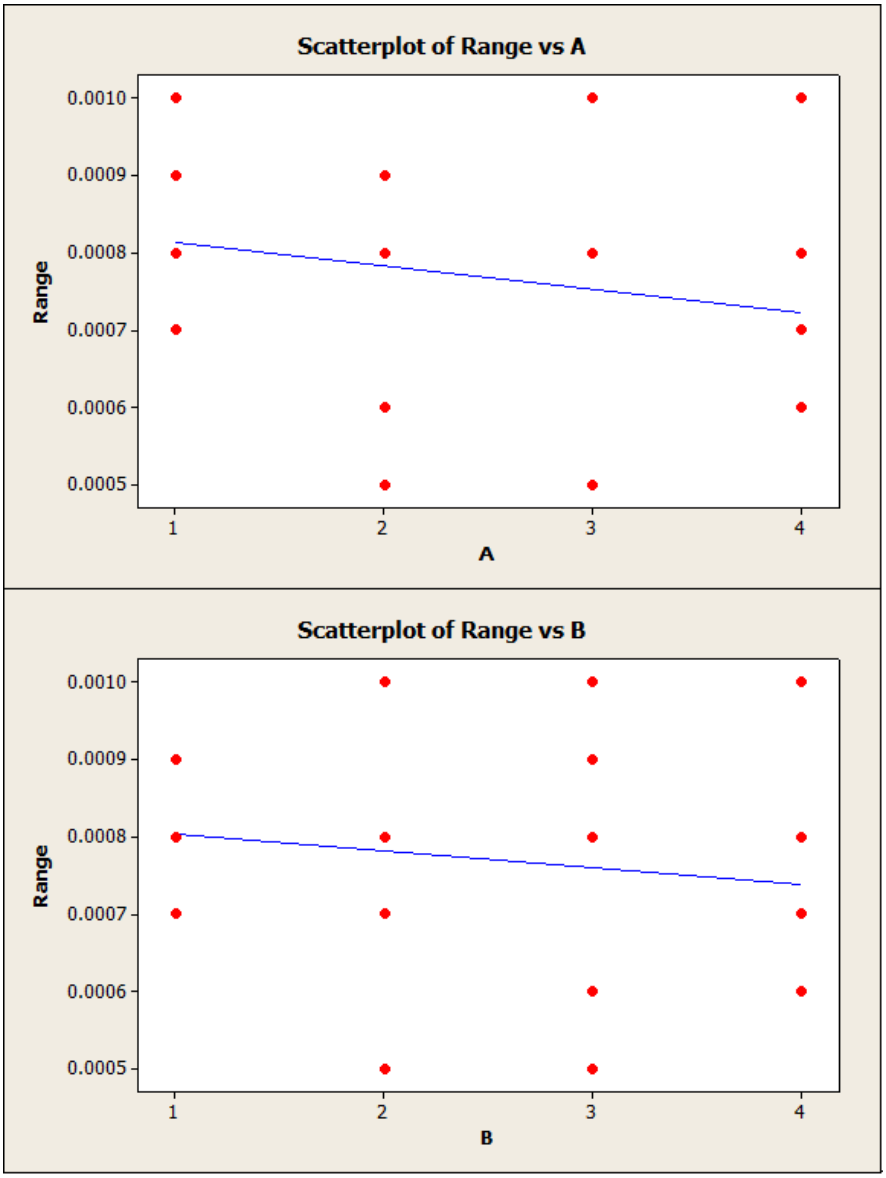

FIGURE 17. PLOTS OF CONTACT VS. RANGE VALUES

The comparison in Trial A features an R-sq value of 4.3% and in Trial B, 1.9%, confirming initial thoughts that there was little to no correlation between the range and amount of contact observed.

This lack correlation between range and contact is to be expected due to the range values not considering the contact across the entire coupling. One might expect to see more transfer across teeth with a small range value due to the two surfaces having contours that are more similar than would be seen with a large range. This does not however incorporate the primary determining factor of tooth contact, the absolute position of the surfaces with relation to the entire coupling as a whole. This primary factor is shown in the "Z-coord" plot, and as the resulting R-sq values show, there is correlation between contact and separation of surfaces

Sorted tables of these comparisons can be found in Appendix A.

4.2 Conclusion

While the methods described in this paper are unable to provide a digital method for the inspection of fixed CURVIC coupling contact pattern, there does appear to be correlation between certain aspects of the results; most notably the correlation between average Z-value of the subtraction mesh and the amount of marking compound transferred.

Further investigation of this matter could benefit from the use of CURVIC couplings produced by Gleason grinders and designed for actual use. Should resources permit it, a more precise and flow friendly type of measurement device could also replace the CMM used in this investigation. The relatively small sample size of points (25) from the tactile

probing with the CMM does not provide the resolution needed to determine the characteristics of contact pattern across an individual tooth.

Analysis at all possible combinations of rotational orientations between the two couplings could be investigated, whereas in this paper only one particular orientation was analyzed. This provides an interesting opportunity for future applications of a digital method to be able to quickly identify which rotational orientation provides the best contact by performing computerized calculations rather than repeating physical tests at large rotational increments that will most likely not be performed at the optimal orientation, particularly when the number of teeth is high.

To better facilitate any sort of future validation of a digital inspection method a more clearly defined scale of transfer characteristics to describe the patterns seen with current marking compound inspection would be helpful. The development of such a scale would also immediately increase traceability and provide a foundation to reduce variation in interpretations between operators.

BIBLIOGRAPHY

1. Bracci, Gabiccini, Artoni, Guiggiani. “Geometric contact pattern estimation for gear drives.” *Comput. Methods Appl. Mech. Engrg.*, 198 (2009): 1563-1571
2. The Gleason Works, *CURVIC Coupling Design*, Rochester, New York, 1973
3. The Gleason Works, *CURVIC Coupling Dimension Sheet Explanations,* Rochester, New York, 1973
4. The Gleason Works, *CURVIC Coupling Inspection*, Rochester, New York, n.d.
5. The Gleason Works, *Fixed CURVIC Coupling*, Rochester, New York, 1979
6. The Gleason Works, *Understanding Tooth Contact Analysis*, Rochester, New York, 1981
7. Goch. “Gear Metrology.” *CIRP Annals – Manufacturing Technology,* 52.2 (2003): 659-695
8. Hsu. “A Study on the CAD/CAM of CURVIC Couplings.” *Proceedings – ASME Turbo Expo 2002: Power for Land, Sea, and Air,* (GT2002): 1157-1162
9. Litvin, Chen, Seol, Kim, Lu, Zhao, and Handschuh. “Computerized Design and Generation of Gear Drives With a Localized Bearing Contact and a Low Level of Transmission Errors.” *NASA TM—102750*, 1996
10. Litvin, Sheveleva, Vecchiato, Gonzalez-Perez, Fuentes. “Modified approach for tooth contact analysis of gear drives and automatic determination of guess values.” *Comput. Methods Appl. Mech. Engrg.*, 194 (2005): 2927-29406
11. Lotze, Haertig. “3D gear measurement by CMM.” *Laser Metrology and Machine Performance V*, WIT Press, Southampton, (2001): 333-344

12. Mathia, Pawlus, Wieczorowski. “Recent trends in surface metrology.” *Wear*, 271 (2011): 494-508
13. Orchard. “Inspection of curvic couplings using a CMM.” *Transactions on Engineering Sciences,* 44 (2003): 222-230
14. Richardson. “A validation of the three-dimensional finite element contact method for use with Curvic couplings.” *Proceedings – Institution of Mechanical Engineers, Part G: Journal of Aerospace Engineering,* 216 (2002): 63-75
15. Savio, De Chiffre, Schmitt. “Metrology of freeform shaped parts.” *CIRP Annals – Manufacturing Technology*, 56.2 (2007): 810-835
16. Vincent, Dantan, Bigot. “Virtual meshing simulation for gear conformity verification.” *CIRP Journal of Manufacturing Science and Technology*, 2.1 (2009): 35-46

APPENDIX

Sorted Comparisons

Z-Coord Smallest to Largest

Int	Z-Coord	Range	Trial A	Trial B
14	-0.00450	0.0008	Full Transfer	Full Transfer
16	-0.00425	0.0010	Significant transfer across center	Full Transfer
12	-0.00410	0.0010	Full Transfer	Full Transfer
2	-0.00380	0.0006	Full Transfer	Full Transfer
7	-0.00375	0.0008	Full Transfer	Full Transfer
18	-0.00375	0.0010	No Transfer	Slight transfer across center
24	-0.00375	0.0006	Full Transfer	Full Transfer
9	-0.00366	0.0007	Full Transfer	Full Transfer
10	-0.00350	0.0008	Significant transfer across center	Significant transfer across center
11	-0.00350	0.0010	Significant transfer across center	Significant transfer across center
20	-0.00350	0.0007	No Transfer	Slight transfer across center
22	-0.00350	0.0010	Significant transfer across center	Significant transfer across center
5	-0.00333	0.0006	Slight transfer across center	Significant transfer across center
19	-0.00333	0.0006	Full Transfer	Full Transfer
4	-0.00325	0.0005	Significant transfer across center	Slight transfer towards outside edge
21	-0.00325	0.0006	Full Transfer	Full Transfer
1	-0.00300	0.0009	Slight transfer towards inside edge	Significant transfer across center
8	-0.00300	0.0008	No Transfer	No Transfer
13	-0.00300	0.0005	Significant transfer across center	Significant transfer across center
15	-0.00300	0.0008	Slight transfer across center	Slight transfer across middle
17	-0.00300	0.0005	Slight transfer across center	Significant transfer across center
6	-0.00290	0.0009	No Transfer	No Transfer
23	-0.00275	0.0007	No Transfer	No Transfer
3	-0.00266	0.0009	No Transfer	No Transfer

Range Smallest to Largest

Int	Z-Coord	Range	Trial A	Trial B
4	-0.00325	0.0005	Significant transfer across center	Slight transfer towards outside edge
13	-0.00300	0.0005	Significant transfer across center	Significant transfer across center
17	-0.00300	0.0005	Slight transfer across center	Significant transfer across center
2	-0.00380	0.0006	Full Transfer	Full Transfer
24	-0.00375	0.0006	Full Transfer	Full Transfer
5	-0.00333	0.0006	Slight transfer across center	Significant transfer across center
19	-0.00333	0.0006	Full Transfer	Full Transfer
21	-0.00325	0.0006	Full Transfer	Full Transfer
9	-0.00366	0.0007	Full Transfer	Full Transfer
20	-0.00350	0.0007	No Transfer	Slight transfer across center
23	-0.00275	0.0007	No Transfer	No Transfer
14	-0.00450	0.0008	Full Transfer	Full Transfer
7	-0.00375	0.0008	Full Transfer	Full Transfer
10	-0.00350	0.0008	Significant transfer across center	Significant transfer across center
8	-0.00300	0.0008	No Transfer	No Transfer
15	-0.00300	0.0008	Slight transfer across center	Slight transfer across middle
1	-0.00300	0.0009	Slight transfer towards inside edge	Significant transfer across center
6	-0.00290	0.0009	No Transfer	No Transfer
3	-0.00266	0.0009	No Transfer	No Transfer
16	-0.00425	0.0010	Significant transfer across center	Full Transfer
12	-0.00410	0.0010	Full Transfer	Full Transfer
18	-0.00375	0.0010	No Transfer	Slight transfer across center
11	-0.00350	0.0010	Significant transfer across center	Significant transfer across center
22	-0.00350	0.0010	Significant transfer across center	Significant transfer across center